Enhanced interfacial Dzyaloshinskii-Moriya interactions in annealed Pt/Co/MgO structures

PAPER

Enhanced interfacial Dzyaloshinskii—Moriya interactions in annealed Pt/Co/MgO structures

IOP Publishing Nanotechnology
Nanotechnology 31 (2020) 155705 (7pp) https://doi.org/10.1088/1361-6528/ab62cd

Enhanced interfacial Dzyaloshinskii—Moriya interactions in annealed Pt/Co/MgO structures

Anni Cao[1,2], Runze Chen[1], Xinran Wang[1], Xueying Zhang[1,3], Shiyang Lu[4], Shishen Yan[4], Bert Koopmans[2] and Weisheng Zhao[1,3]

[1] Fert Beijing Institute, BDBC, School of Microelectronics, Beihang University, Beijing 100191, People's Republic of China
[2] Department of Applied Physics, Institute for Photonic Integration, Eindhoven University of Technology, PO Box 513, 5600 MB Eindhoven, The Netherlands
[3] Beihang-Goertek Joint Microelectronics Institute, Qingdao Research Institute, Beihang University, Qingdao 266104, People's Republic of China
[4] School of Physics, State Key laboratory of Crystal Materials, Shandong University, Jinan 250100, People's Republic of China

E-mail: weisheng.zhao@buaa.edu.cn

Received 26 August 2019, revised 14 November 2019
Accepted for publication 17 December 2019
Published 24 January 2020

Abstract

The interfacial Dzyaloshinskii−Moriya interaction (iDMI) is attracting great interest for spintronics. An iDMI constant larger than 3 mJ m^{-2} is expected to minimize the size of skyrmions and to optimize the domain-wall dynamics. In this study, we experimentally demonstrate a giant iDMI in Pt/Co/X/MgO ultra-thin film structures with perpendicular magnetization. The iDMI constants were measured using a field-driven creep regime domain expansion method. The enhancement of iDMI with an atomically thin insertion of Ta and Mg is comprehensively understood with the help of *ab-initio* calculations. Thermal annealing has been used to crystallize the MgO thin layer to improve the tunneling magneto-resistance (TMR), but interestingly it also provides a further increase of the iDMI constant. An increase of the iDMI constant of up to 3.3 mJ m^{-2} is shown, which is promising for the scaling down of skyrmion electronics.

Supplementary material for this article is available online

Keywords: Dzyaloshinskii−Moriya interaction (DMI), inserted layer, annealing, domain-walls (DW)

(Some figures may appear in colour only in the online journal)

Introduction

The Dzyaloshinskii−Moriya interaction (DMI) is an anti-symmetric exchange interaction that appears in inversion asymmetric structures and which leads to chiral spin texture. In most of the magnetic thin films, the interfacial DMI (iDMI), as the dominant contribution of DMI, is one of the key ingredients for magnetic skyrmions [1–4] and chiral domain-walls (DWs) [5–7]. It has been intensively studied in the past few years, and has been reported to influence the DW spin structures [8] and their current-driven dynamics [5, 6, 9, 10]. Moreover, the DMI is responsible for establishing and controlling the size of magnetic skyrmions [11]. These small chiral spin textures are promising potential information carriers in future non-volatile spintronic applications, due to their unique properties including propagation driven by ultralow current densities [12–14] and re-writability using spin-polarized currents [15]. Although some theoretical and experimental efforts have been devoted to unveiling the mechanism of DMI, it is still elusive, particularly in non-

epitaxial sputtered thin films. In systems of interest for spintronic applications, a strong DMI is urgently needed to overcome the exchange interaction and destabilize the uniform ferromagnetic state. Therefore, manipulating DMI efficiently is a crucial task for the development of advanced memory devices [16].

Our previous study [17] has proven that insertion of a 'dusting' Mg layer in a Pt/Co/MgO system can prevent the deterioration of the Co/MgO interface during the deposition, further facilitating better crystallization for both the ferromagnetic and insulating layers. In this paper, we propose the use of Ta as an alternative inserted material and explore the role of thermal annealing to further enhance the DMI. Experimental results with first principle calculations are compared to explain why Ta, as the inserted layer, gives rise to slightly higher iDMI energy than Mg does. We also experimentally unveil a relationship between the DMI and thermal annealing. The effective DMI fields of annealed samples were quantified by analyzing the domain-wall motion in the presence of an in-plane field. All of the samples exhibit an annealing-temperature-dependent DMI, which firstly increases and tends to decrease in the end. To the best of our knowledge, this is the first report of a DMI constant for Pt/Co/MgO multilayers of over 3 mJ m^{-2}.

Sample preparation and basic characterization

We use magnetron sputtering at room temperature to deposit multilayers with composition Ta(3 nm)/Pt(4 nm)/Co(1 nm)/X(0.2 nm)/MgO(t)/Pt(5 nm), as shown in figure 1(a). The inserted layer X is designed to be Ta or Mg, while the MgO thickness, *t*, varies from 0 to 2.0 nm. The inserted layer X is used for protecting the Co from excessive oxidation. Moreover, we hope to strengthen the DMI through this layer. Samples with different MgO thicknesses were also prepared to examine the variance of DMI. The top Pt provides a protective layer preventing the film from oxidation.

A sectional view using a spherical aberration corrected transmission electron microscope (TEM) is shown in the insertion of figure 1(a) for the Pt/Co/Ta/MgO (1.2 nm) sample. Referring to the nominal thickness, we indicate the approximate borders of each layer with red dashed lines. The clear Pt lattice proves the success of milling using the focused ion beam (FIB) and the high quality of our multilayers. We use an alternating gradient field magnetometer (AGFM) to confirm the perpendicular magnetization and characterize the magnetic properties of the samples with the two different inserted layers at room temperature. The hysteresis loops for the perpendicular applied field are depicted in figure 1(b). The saturation magnetizations of samples with Ta inserted are slightly higher than the group of samples inserted with Mg. We think the reason could be that the deposited Ta layer is more compact than the Mg layer and that the Ta atomic mass is larger than that of the Mg. The quality of the inserted layer directly influences the intermixing between the Co and MgO

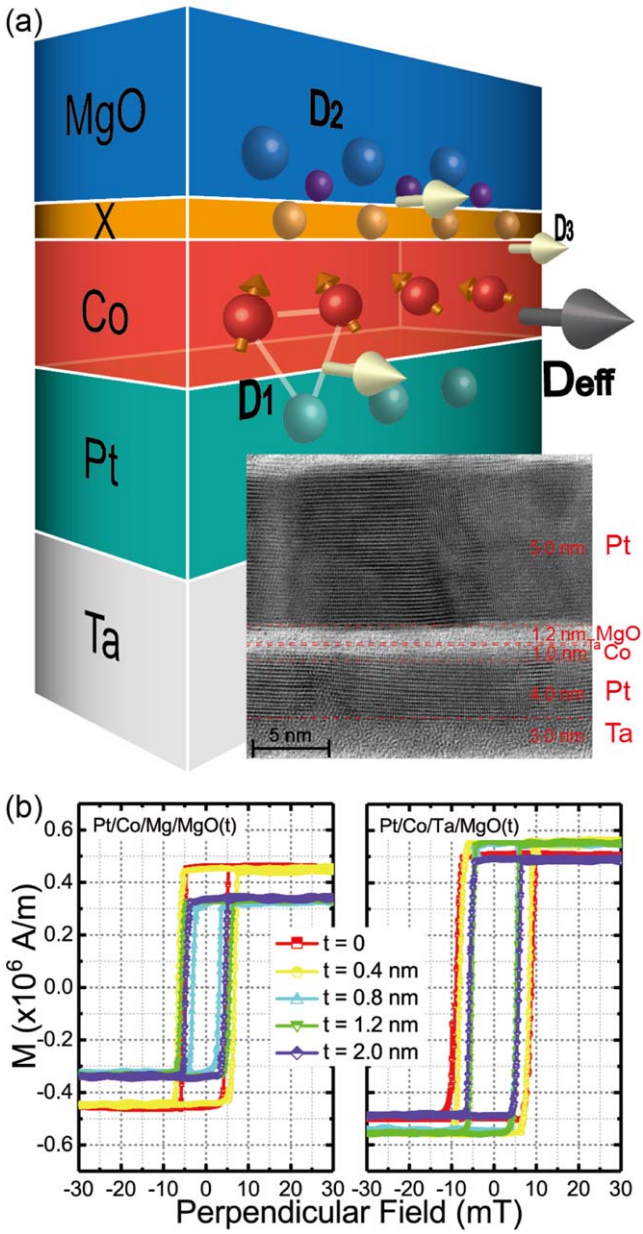

Figure 1. (a) Schematic of the Ta/Pt/Co/X/MgO stack structure. The inserted sub-figure is a cross profile of the as-deposited Pt/Co/Ta/MgO sample with MgO thickness = 1.2 nm as measured by transmission electron microscopy. (b) Hysteresis loops with perpendicular applied field for Pt/Co/Mg/MgO(t) and Pt/Co/Ta/MgO(t) structures.

layer. Results of in-plan loops can be found in figure S1 of the supplementary information, available online at stacks.iop.org/NANO/31/155705/mmedia.

We quantified the strength of DMI in our samples, employing a Kerr microscope to observe asymmetric DW movement in the creep regime with an in-plane field H_X and a perpendicular field H_Z. The dependence of DW velocities on the in-plane field is found to be roughly quadratic, where the minimum occurs at a non-zero value of H_X, which is defined as the effective DMI field H_{DMI} [18–20]. For typical examples

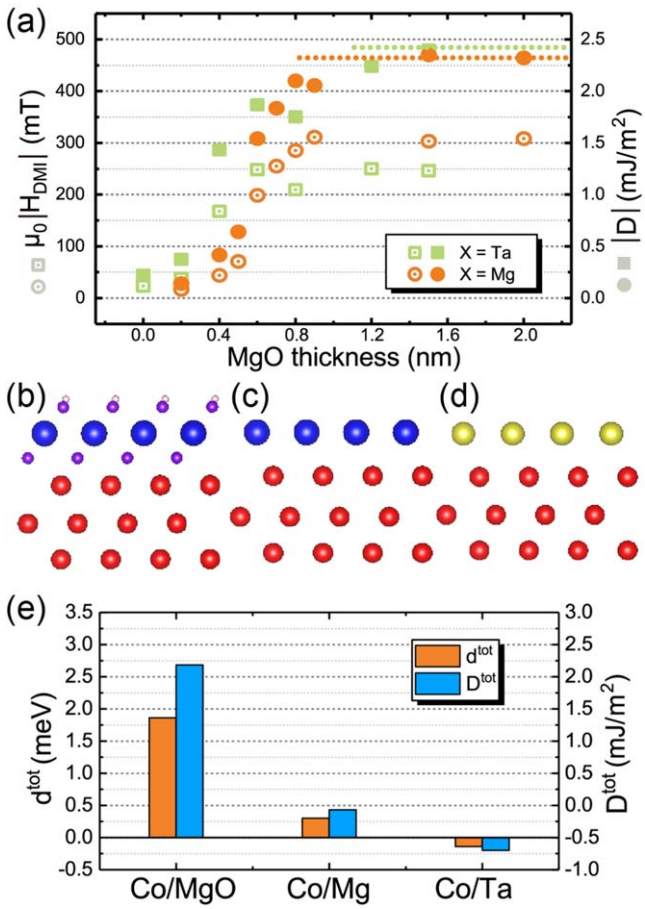

Figure 2. (a) Experimental trends of the effective DMI field $\mu_0|\boldsymbol{H_{DMI}}|$ and DMI constant $|\boldsymbol{D}|$ as a function of MgO thickness with different inserted layer X. Symbols with center dot represent $\mu_0|\boldsymbol{H_{DMI}}|$ and solid symbols represent $|\boldsymbol{D}|$. The ideal interfacial array of atoms used for the first principle calculation, (b) Co/MgO, (c) Co/Mg and (d) Co/Ta. (e) The total DMI strength $\boldsymbol{d^{tot}}$ and the micro-magnetic DMI energy $\boldsymbol{D^{tot}}$ of the three kinds of interfaces.

see figures S2–S4 in the supplementary information. From the DMI field H_{DMI} one can extract the DMI constant

$$|D| = \mu_0 M_S |H_{DMI}| \sqrt{A/K_{eff}}, \quad (1)$$

using values of M_S and K_{eff} as obtained from the measured hysteresis loops, and A from literature. For more details on the operation and analysis see our previous work [17]. Figure 2(a) exhibits the experimental results of DMI for as-deposited samples inserted by Mg and Ta, with various MgO thickness. It can be deduced that DMI almost remain unchanged with the increment of MgO thickness beyond a certain saturation level (1.2–2.0 nm here). Samples with a Pt/Co/Ta/MgO structure and those with a Pt/Co/Mg/MgO structure are found to have approximately the same saturation value of the DMI constant $|D|$, as shown in figure 2(a). First-principle calculations were adopted to judge the performance of Ta and Mg on DMI and to give a reasonable physical explanation.

First-principle calculations

We use *ab initio* calculations to compare the DMI of the Pt/Co/MgO structure after inserting Mg and Ta. One has to realize that the total DMI is a sum of contributions due to the Pt/Co and Co/X/MgO interface, as will be discussed later in more detail. From the calculations we extract the additional DMI from the Co/X/MgO interface. As a comparison, the DMI coefficient of the Co/MgO interface is also calculated. The DMI energy (E_{DMI}) can be depicted as

$$E_{DMI} = \sum_{\langle i,j \rangle} d_{ij} \cdot (S_i \times S_j), \quad (2)$$

where S_i and S_j are nearest neighboring normalized spins and d_{ij} is the corresponding DMI vector. The total DMI strength d^{tot}, introduced according to $d^{tot} = (E_{CW} - E_{ACW})/12$ [21], can be calculated by identifying the difference between the clockwise energy E_{CW} and anticlockwise energy E_{ACW} (as defined in [22]) based on the density functional theory (DFT). The DMI strength can also be expressed by the micro magnetic energy per volume unit of the magnetic film with the corresponding coefficient D^{tot}. We can write D^{tot} as $D^{tot} = \frac{3\sqrt{2}\,d^{tot}}{2N_F r^2}$, in which r is the distance between two nearest neighbor Co atoms and N_F is the number of the magnetic atomic layers [21].

The VASP package [22, 23] was employed using supercells with a monolayer (ML) of MgO on 3 ML of Co with the surface of MgO passivated by hydrogen, as well as a ML of Mg or Ta on 3ML of Co (figures 2(b)–(d)).

It has been calculated in [34] that the DMI energies at Pt/Co and Co/MgO interfaces are comparable, and we assume that the DMI energy at the Pt/Co interface is not affected by changing the inserted layer X. Considering the interfacial structure for multilayers grown by magnetron sputtering, the inserted monolayer is more likely not to be a closed layer but formed by a distribution of 'islands' between the Co and MgO. Figures 2(b)–(d) show the ideal interfacial atomic structure used for the DMI constant calculation for Co/MgO, Co/Mg and Co/Ta, respectively. In figure 2(e), the total DMI coefficients d^{tot} and the micro-magnetic DMI energy D^{tot} for the three structures are compared. The values of Co/Mg (0.30 meV) and Co/Ta (−0.14 meV) are found to be much smaller than those of Co/MgO (1.86 meV). To some extent this indicates that bringing additional DMI is not the dominant function of the inserted layer. Rather, since the *ab-initio* calculations predict that DMI should reduce at atomic locations where a closed layer of X forms, this means that at places where the interface can be considered as Co/MgO-like (without X), i.e. at places where Co–O bonds dominate, the DMI should have increased. Therefore, we conjecture that insertion of Ta and Mg makes the pristine interface better, i.e., it overcompensates the loss of DMI by the presence of Ta or Mg. Based on the opposite sign of D^{tot} for Ta and Mg, this effect should be stronger for Ta than for Mg, since the calculated reduction of DMI for Ta is larger than for Mg. In this way, Ta is slightly better than Mg in enhancing the DMI

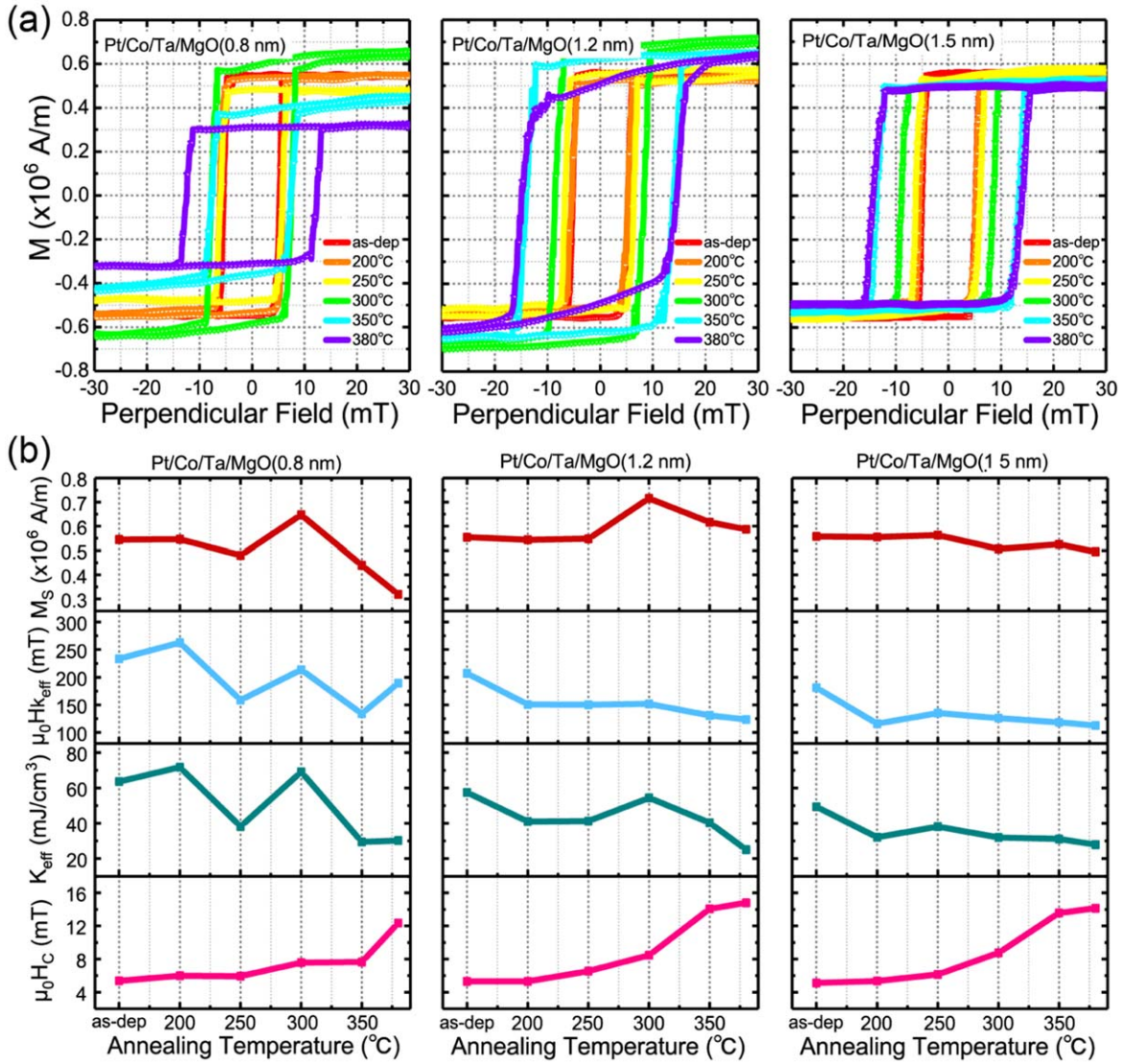

Figure 3. (a) Hysteresis loops applied with perpendicular field of annealed Pt/Co/Ta/MgO(t) structures while t = 0.8 nm, 1.2 nm and 1.5 nm. Different annealing temperatures of the samples with the same structure are distinguished by different color in each subfigure. (b) Magnetic properties obtained from the hysteresis loops for samples with different annealing temperatures. The subfigures in each line share common scales and y-axis legends shown on the left.

energy of the Pt/Co/MgO system. A valance state analysis of Co with different insertion layers could be another interesting method to explain the role of the inserted layer quantitatively, but we are not going to involve this subtle issue in this paper.

Annealing effects on magnetic properties

Different samples were annealed for half an hour at temperatures ranging up to 380 °C, after which the hysteresis loops and DW motion were measured at room temperature. We controlled the rising rate and the duration of annealing temperatures so that they remained the same, and applied a 50 mT perpendicular field while annealing. Hysteresis loops with perpendicular magnetic field for the annealed samples with Ta inserted are shown in figure 3(a), for MgO thicknessess $t = 0.8$, 1.2 and 1.5 nm. The corresponding in-plane field loops can be found in the supplementary information as figure S1. The sharp switching of the magnetization in the perpendicular loops are consistent with perpendicular anisotropy of all samples, although some details of the loops depend on thermal annealing. Figure 3(b) shows the magnetic properties extracted from the hysteresis loops for samples with different annealing temperatures. We observe that the saturation magnetization M_S of the sample with the thickest MgO shows hardly any dependence on annealing, whereas for the thinnest oxide sample there is a trend of an initial increase followed by a decrease. The effective anisotropy field $H_{k_{eff}}$ was obtained by extracting the field corresponding to 90% of the saturated magnetization in the hysteresis loops with in-plane magnetic field. As the annealing temperature rises from 200 °C to 380 °C, $H_{k_{eff}}$ shrinks to 60% upon annealing. The effective magnetic anisotropy energy K_{eff}, calculated as $K_{eff} = \frac{1}{2}\mu_0 H k_{eff} M_S$ [24, 25], shows similar

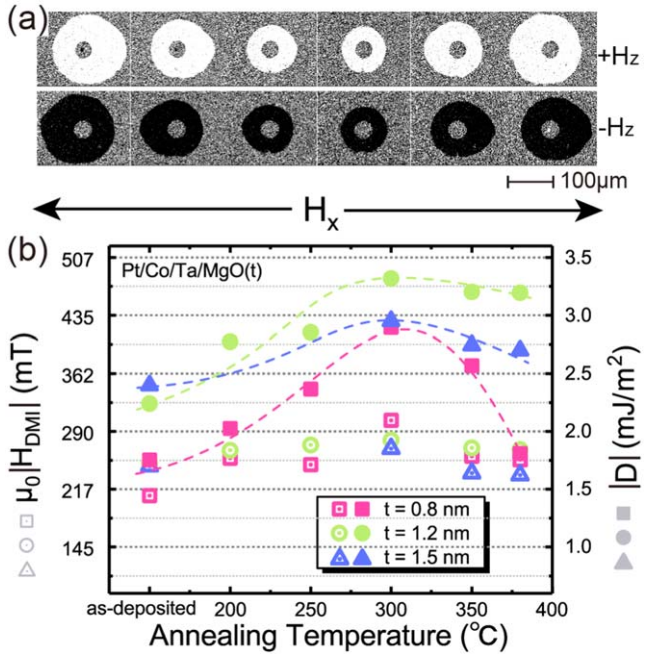

Figure 4. (a) DW expansion of the same sample driven by an out-of-plane magnetic field $\mu_0|\boldsymbol{H}_z| = 10.62$ mT and a varying in-plane field $\mu_0\boldsymbol{H}_x$. (b) Trends of the effective DMI field and DMI constant as a function of annealing temperature. Square symbols, circular symbols and triangle symbols stand for the MgO thickness $t = 0.8$ nm, 1.2 nm and 1.5 nm separately. Symbols with center dot stand for $\mu_0|\boldsymbol{H}_{DMI}|$ while those solid ones stand for $|\boldsymbol{D}|$.

trends as M_S. With the increase of annealing temperature, the coercive field H_C exhibits a 3–4 times growth compared with the as-deposited samples, which is consistent with previous studies [26]. Overall we find quite similar trends in the magnetic properties upon annealing Pt/Co/Ta/MgO samples with different MgO thickness.

Annealing effcts on dmi

A typical result of asymmetrical DW motions in the presence of an in-plane field for two directions of the out of plane field $\mu_0 H_z$ is shown in figure 4(a). The applied $\mu_0 H_z$ which varies from several milli-tesla to tens of milli-tesla for different samples, and the in-plane field $\mu_0 H_x$ was in the range of ± 350 mT. A selection of our DW velocity measurements can be found in figures S2 to S4. We verified that domain-wall motion is in the creep regime for all perpendicular fields applied, as shown in figures S5 to S7 in the supplementary material. Thus, an unambiguous value of the DMI parameter is obtained for each sample at each annealing temperature. The absolute value of the DMI constant $|D|$ can be calculated with equation (1) [27]. By assuming the exchange stiffness constant $A = 15$ pJ m^{-1} [28, 29], our $|D|$ can reach as high as 3.3 mJ m^{-2}. We are aware that the assessment of the exchange stiffness A is not trivial, since the annealing process is quite likely to have an effect on it. Although the temperature dependence was directly ignored in some literatures [26, 30], other work has suggested an increasing exchange stiffness with increasing annealing temperature in similar thin films [31, 32]. The latter suggestion might mean that our estimate of DMI would be a conservative estimate, and its actual value could be higher. The effective DMI fields $\mu_0|H_{DMI}|$ and DMI energy $|D|$ for three components Pt/Co/Ta/MgO (0.8 nm, 1.2 nm and 1.5 nm) assuming a constant A are depicted in figure 4(b). We thus found that the strength of DMI manifests in differences for different MgO thickness, but they all exhibit a trend of an initial increase followed by a decrease. Within the investigated range, the DMI values display an optimum at an annealing temperature of around 300 °C, independent of the MgO thickness.

Discussion

In the Pt/Co/MgO system, the large interfacial DMI $iDMI_{Pt/Co/MgO}$ does not only come from the strong spin orbit coupling (SOC) between the Pt and Co, but also has a significant contribution from the Co/MgO interface, following the expression $iDMI_{Pt/Co/MgO} = iDMI_{Pt/Co} + iDMI_{Co/MgO}$. The DFT calculations have proven that $iDMI_{Pt/Co}$ and $iDMI_{Co/MgO}$ have the same sign [33]. It has been accepted that interfacial oxidation is related to large charge transfer and to the large interfacial electric field that compensates the small spin–orbital coupling of the atoms at the interface, which directly increase the DMI [34, 35]. The inserted X layer efficiently protects the Co layer from degradation, and a proper material could strengthen the asymmetry of the whole structure, and consequently enhance the DMI.

It was reported that the annealing process would homogenize the oxide layer [36, 37], and improve the Co/MgO interface, though there has not been a layer X inserted between the Co and MgO in former studies. To confirm this, another TEM image is provided in figure 5(a). Compared with figure 1(a), the degrees of crystallinity for Co and MgO layers are appreciably improved. We also exhibit a comparison of x-ray energy dispersive spectroscopy curves for the Pt/Co/Ta/MgO (1.2 nm) sample before and after 300 °C thermal annealing in figure 5(b), where the curves are shifted such that the Co peak positions defined the zero position of the scan. The O atoms' peak position shows a small, but finite 5% shift for the annealed sample, which would be consistent with the slight growth of M_S for the 300 °C annealed sample (seen as figure 3(e)). Secondly, an improved ordering of the atoms at the Pt/Co interface, which is brought about by annealing, might be another reason for the initial enhancement of the DMI, since the DMI is sensitive to the atomic arrangements at the interface [10, 38]. Following the increasing trend, a higher temperature will prompt the formation of a CoPt alloy at the Pt/Co interface and reduces the number of Co–O bonds [37]. Furthermore, it was reported [21] that annealing at higher temperatures leads to interfacial diffusion, being detrimental for the DMI. Therefore, a decreasing trend of DMI appears when the temperature goes above 300 °C. A similar trend was also found in Ta/CoFeB/MgO tri-layers [39]. Above all, the non-monotonic trend of DMI can be explained rationally.

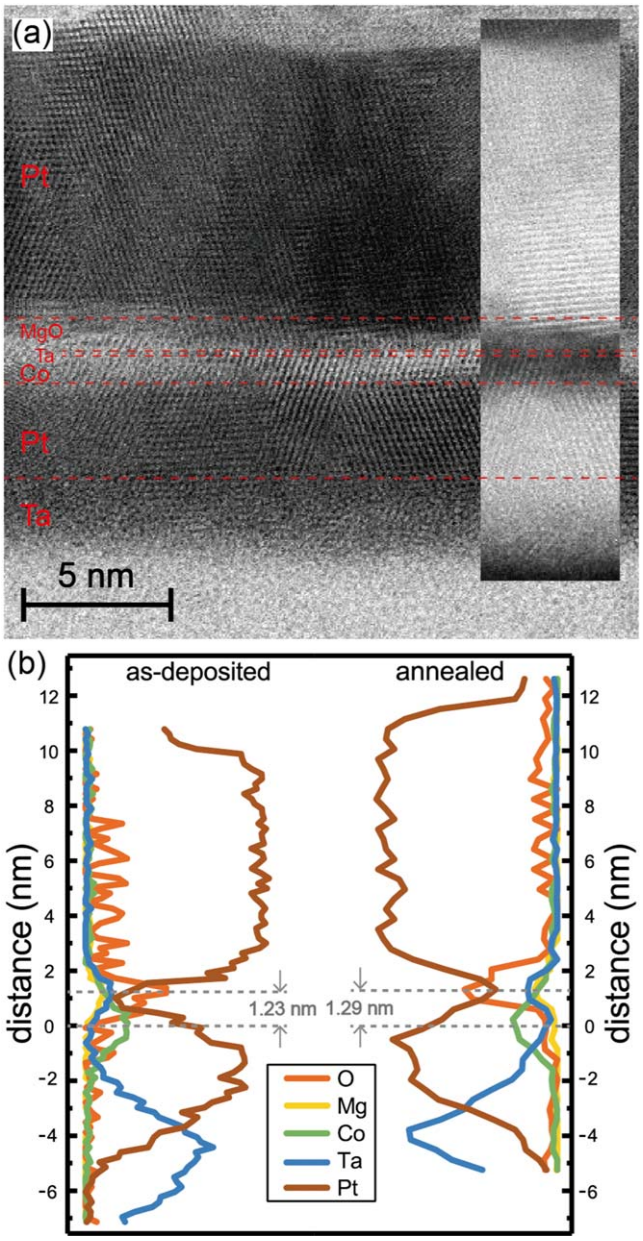

Figure 5. (a) Cross profile of the Pt/Co/Ta/MgO (1.2 nm) sample after annealing at 300 °C as measured by transmission electron microscopy. The inserted subfigure is the result with an inverted imaging field. (b) X-ray energy dispersive spectroscopy curves of the as-deposited sample and the 300 °C annealed sample.

The Pt/Co/MgO structure we studied here is very similar to the configuration of a tunnel barrier layer/free layer/capping layer of the most popular magnetic tunnel junction (MTJ) structure [40]. Thermal annealing is a necessary method to produce a crystallized MgO tunnel barrier, thus improving the tunneling magnetoresistance (TMR) effect in magnetic multilayers [41]. Therefore, our study will be very relevant for applications that make use of the electrical detection of magnetic skyrmions through TMR in MTJ devices. Further improvement of the lattice on asymmetric interface by thermal annealing is an essential way to fine-tune the DMI in Pt/Co/MgO samples which is valuable for the induction of chiral magnetic order.

Conclusion

In summary, using a combined experimental and theoretical study, we prove that insertion of both X = Ta and Mg in Pt/Co/X/MgO structures improves DMI significantly, while the effect on the interface quality may be slightly better for Ta than for Mg. Furthermore, we investigated the effect of thermal annealing on the DMI. Benefiting from the optimization of interfaces, a significantly enhanced iDMI is found in our annealed Pt/Co/Ta/MgO system. The optimal condition for the Pt/Co/Ta/MgO structure is found to be annealing around 300 °C, for 0.5 h, enhancing DMI to the largest extent. The influence of annealing is attributed to both Pt/Co and Co/MgO interface transformation. Our study will significantly contribute to research that relies on strong DMI in thin film systems, and to stabilize magnetic skyrmions at room-temperature.

Acknowledgments

The authors would like to thank the support for the project from the National Natural Science Foundation of China (No.61627813 and 61571023), the National Key Technology Program of China (2017ZX01032101), the Program of Introducing Talents of Discipline to Universities in China (No. B16001), the VR innovation platform from the Qingdao Science and Technology Commission and the China Scholarship Council.

ORCID iDs

Weisheng Zhao https://orcid.org/0000-0001-8088-0404

References

[1] Hou Z *et al* 2017 Observation of various and spontaneous magnetic skyrmionic bubbles at room temperature in a frustrated kagome magnet with uniaxial magnetic anisotropy *Adv. Mater.* **29** 1–8
[2] Zhang X *et al* 2018 Skyrmions in magnetic tunnel junctions *ACS Appl. Mater. Interfaces* **10** 16887–92
[3] Yu X Z, Onose Y, Kanazawa N, Park J H, Han J H, Matsui Y, Nagaosa N and Tokura Y 2010 Real-space observation of a two-dimensional skyrmion crystal *Nature* **465** 901–4
[4] Sampaio J, Cros V, Rohart S, Thiaville A and Fert A 2013 Nucleation, stability and current-induced motion of isolated magnetic skyrmions in nanostructures *Nat. Nanotechnol.* **8** 839–44
[5] Ryu K-S, Thomas L, Yang S-H and Parkin S 2013 Chiral spin torque at magnetic domain walls *Nat. Nanotechnol.* **8** 527–33
[6] Emori S, Bauer U, Ahn S M, Martinez E and Beach G S D 2013 Current-driven dynamics of chiral ferromagnetic domain walls *Nat. Mater.* **12** 611–6
[7] Zhang X, Vernier N, Zhao W, Yu H, Vila L and Zhang Y 2018 Direct observation of domain-wall surface tension by deflating or inflating a magnetic bubble *Phys. Rev. Appl.* **9** 024032

[8] Benitez M J, Hrabec A, Mihai A P, Moore T A, Burnell G, Mcgrouther D, Marrows C H and McVitie S 2015 Magnetic microscopy and topological stability of homochiral Néel domain walls in a Pt/Co/AlO x trilayer *Nat. Commun.* **6** 1–7

[9] Thiaville A, Rohart S, Jué É, Cros V and Fert A 2012 Dynamics of Dzyaloshinskii domain walls in ultrathin magnetic films *Europhys. Lett.* **100** 57002

[10] Hrabec A, Porter N A, Wells A, Benitez M J, Burnell G, McVitie S, McGrouther D, Moore T A and Marrows C H 2014 Measuring and tailoring the Dzyaloshinskii-Moriya interaction in perpendicularly magnetized thin films *Phys. Rev.* B **90** 020402

[11] Nagaosa N and Tokura Y 2013 Topological properties and dynamics of magnetic skyrmions *Nat. Nanotechnol.* **8** 899–911

[12] Jiang W, Upadhyaya P, Zhang W, Yu G, Jungfleisch M B, Velthuis S G E and Hoffmann A 2015 Blowing magnetic skyrmion bubbles *Science (80-.)* **349** 283–6

[13] Schulz T, Ritz R, Bauer A, Halder M, Wagner M, Franz C, Pfleiderer C, Everschor K, Garst M and Rosch A 2012 Emergent electrodynamics of skyrmions in a chiral magnet *Nat. Phys.* **8** 301–4

[14] Iwasaki J, Mochizuki M and Nagaosa N 2013 Current-induced skyrmion dynamics in constricted geometries *Nat. Nanotechnol.* **8** 742–7

[15] Romming *et al* 2013 The frequency shift, lineshape, and Ramsey fringe contrast are quantities that all depend on the first-order expectation values of the spin operators % *Science (80-.)* **341** 636–9

[16] Parkin S S P, Hayashi M and Thomas L 2008 Magnetic domain-wall racetrack memory *Science (80-.)* **320** 190–4

[17] Cao A, Zhang X, Koopmans B, Peng S, Zhang Y, Wang Z, Yan S, Yang H and Zhao W 2018 Tuning the Dzyaloshinskii-Moriya interaction in Pt/Co/MgO heterostructures through the MgO thickness *Nanoscale* **10** 12062–7

[18] Lemerle S, Ferré J, Chappert C, Mathet V, Giamarchi T and Le Doussal P 1998 Domain wall creep in an ising ultrathin magnetic film *Phys. Rev. Lett.* **80** 849–52

[19] Chauve P, Giamarchi T and Le Doussal P 2000 Creep and depinning in disordered media *Phys. Rev.* B **62** 6241–67

[20] Jaiswal S *et al* 2017 Investigation of the Dzyaloshinskii-Moriya interaction and room temperature skyrmions in W/CoFeB/MgO thin films and microwires *Appl. Phys. Lett.* **111** 022409

[21] Yang H, Thiaville A, Rohart S, Fert A and Chshiev M 2015 Anatomy of Dzyaloshinskii-Moriya interaction at Co/Pt interfaces *Phys. Rev. Lett.* **115** 267210

[22] Kresse G and Hafner J 1993 *Ab initio* molecular dynamics for liquid metals *Phys. Rev.* B **47** 558–61

[23] Kresse G and Furthmüller J 1996 Efficient iterative schemes for ab initio total-energy calculations using a plane-wave basis set *Phys. Rev. B—Condens. Matter Mater. Phys.* **54** 11169–86

[24] Yakushiji K, Kubota H, Fukushima A and Yuasa S 2016 Perpendicular magnetic tunnel junction with enhanced anisotropy obtained by utilizing an Ir/Co interface *Appl. Phys. Express* **9** 013003

[25] Johnson M T, Bloemen P J H, den Broeder F J A and de Vries J J 1996 Magnetic anisotropy in metallic multilayers *Reports Prog. Phys.* **59** 1409–58

[26] Schlotter S, Agrawal P and Beach G S D 2018 Temperature dependence of the Dzyaloshinskii-Moriya interaction in Pt/Co/Cu thin film heterostructures *Appl. Phys. Lett.* **113** 1–6

[27] Je S G, Kim D H, Yoo S C, Min B C, Lee K J and Choe S B 2013 Asymmetric magnetic domain-wall motion by the Dzyaloshinskii-Moriya interaction *Phys. Rev. B—Condens. Matter Mater. Phys.* **88** 214401

[28] Metaxas P J, Jamet J P, Mougin A, Cormier M, Ferré J, Baltz V, Rodmacq B, Dieny B and Stamps R L 2007 Creep and flow regimes of magnetic domain-wall motion in ultrathin Pt/Co/Pt films with perpendicular anisotropy *Phys. Rev. Lett.* **99** 217208

[29] Pai C F, Mann M, Tan A J and Beach G S D 2016 Determination of spin torque efficiencies in heterostructures with perpendicular magnetic anisotropy *Phys. Rev.* B **93** 144409

[30] Cho J, Jung J, Cho S and You C 2015 Effect of annealing temperature on exchange stiffness of CoFeB thin fi lms frequency shift (GHz) *J. Magn. Magn. Mater.* **395** 18–22

[31] Vashisht G, Goyal R and Annapoorni S 2018 Exchange stiffness variation for thermally annealed FeCo thin films *AIP Conf. Proc.* **1942** 130017

[32] Belmeguenai M, Gabor M S, Zighem F, Roussign Y, Faurie D and Tiusan C 2016 Annealing temperature and thickness dependencies of structural and magnetic properties of Co_2 FeAl thin films *Phys. Rev.* B **94** 104424

[33] Yang H, Boulle O, Cros V, Fert A and Chshiev M 2018 Controlling Dzyaloshinskii-Moriya interaction via chirality dependent atomic-layer stacking, insulator capping and electric field *Sci. Rep.* **8** 12356

[34] Boulle O *et al* 2016 Room-temperature chiral magnetic skyrmions in ultrathin magnetic nanostructures *Nat. Nanotechnol.* **11** 449–54

[35] Belabbes A, Bihlmayer G, Blügel S and Manchon A 2016 Oxygen-enabled control of Dzyaloshinskii-Moriya Interaction in ultra-thin magnetic films *Sci. Rep.* **6** 1–9

[36] Cho J, Kim N, Jung J, Han D, Swagten H J M, Kim J and You C 2018 Thermal annealing effects on the interfacial Dzyaloshinskii-Moriya interaction energy density and perpendicular magnetic anisotropy *IEEE Trans. Magn.* **54** 1500104

[37] Garad H, Ortega L, Ramos A Y, Joly Y, Fettar F, Auffret S, Rodmacq B, Diény B, Proux O and Erko A I 2013 Competition between CoOx and CoPt phases in Pt/Co/AlO_x semi tunnel junctions *J. Appl. Phys.* **114** 053508

[38] Lavrijsen R, Hartmann D M F, Van Den Brink A, Yin Y, Barcones B, Duine R A, Verheijen M A, Swagten H J M and Koopmans B 2015 Asymmetric magnetic bubble expansion under in-plane field in Pt/Co/Pt: effect of interface engineering *Phys. Rev. B—Condens. Matter Mater. Phys.* **91** 104414

[39] Khan R A, Shepley P M, Hrabec A, Wells A W J, Ocker B, Marrows C H and Moore T A 2016 Effect of annealing on the interfacial Dzyaloshinskii-Moriya interaction in Ta/CoFeB/MgO trilayers *Appl. Phys. Lett.* **109** 132404

[40] Sbiaa R, Meng H and Piramanayagam S N 2011 Materials with perpendicular magnetic anisotropy for magnetic random access memory *Phys. Status Solidi - Rapid Res. Lett.* **5** 413–9

[41] Wang M *et al* 2018 Current-induced magnetization switching in atom-thick tungsten engineered perpendicular magnetic tunnel junctions with large tunnel magnetoresistance *Nat. Commun.* **9** 1–7